

Surface plasmon resonance sensor with a magneto-optical structure

JAROMÍR PIŠTORA¹, MICHAL LESŇÁK¹, ONDŘEJ VLAŠÍN¹, MICHAL CADA²

¹Institute of Physics, VŠB – Technical University of Ostrava,
17. listopadu 15, Ostrava Poruba 708 33, Czech Republic

²Department of Electrical and Computer Engineering, Dalhousie University,
Halifax, Nova Scotia, B3J 2X4, Canada

*Corresponding author: jaromir.pistora@vsb.cz

Due to resonant excitation of surface plasmons, surface plasmon resonance (SPR) sensors combined with ferromagnetic thin films allow an enhancement of the magneto-optical (MO) response. MO-SPR structures with Au/Co/Au sandwiches are theoretically analyzed in transverse configuration by 4×4 matrix algebra. The influence of sandwich film thickness, layer order and Co–Au multilayers on the relative change of the reflectance for *p*-polarized waves is analyzed. The results show the important role of the incidence angle distribution of the reflectance without magnetic ordering on the MO-SPR response. An optimized geometry and a corresponding feedback are discussed.

Keywords: surface plasmon resonance, magneto-optics, induced anisotropy, optical sensors.

1. Introduction

Surface plasmons are collective oscillations of noble metal electron, propagating along a metal and a dielectric interface. The excitation condition of the surface plasmon resonance (SPR) is very sensitive to changes of refractive index (the order of 10^{-5}) of the dielectric medium [1, 2]. This physical principle has been utilized in SPR sensors by physicists, chemists, material scientists and biologists. Several concepts have been described to improve the sensitivity of SPR (*e.g.*, sensors with angular, wavelength, intensity, phase, and polarization modulation) [3]. A relatively new approach is the combination of magneto-optical (MO) activity of the magnetic materials and SPR. The magneto-optic effects in surface plasmon polaritons propagating in thin metallic layers have been analyzed in [4]. An improvement of the detection limit by a factor of three in refractive index changes for a MO-SPR sensor compared with standard SPR sensors was presented in [1]. The authors in [5] show that the best optimization not only depends on the orientation of the magnetic field but

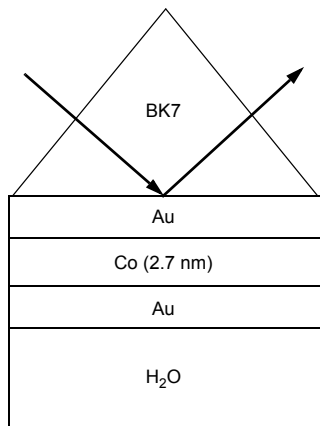


Fig. 1. Geometry of MO-SPR unit.

also on the magneto-optical coefficients. The accurate control of the MO-SPR film thickness is critical in achieving a remarkable increase in MO activity [6]. A large enhancement of the Faraday phenomena by localized surface plasmon resonance in gold nanoparticles embedded in a magnetic garnet film is described in [7]. At present the interest is focused on trilayers (Au–Co–Au, Ag–Co–Ag) and their application in MO-SPR systems. In [8], the authors show that the transverse Kerr signal of Ag–Co–Ag trilayers is strongly affected by the surface plasmon polariton resonance excitation when measured in the Kretschmann configuration. The coupling of an external magnetic field to the surface plasmon-polariton wave vector is greatly enhanced in the Au/Co/Au structure due to the ferromagnetic nature of one of its constituents [9, 10]. The excitation of localized plasmon resonance of an array of Au nanodiscs fabricated on top of Au/Co/Au sandwiches affects the MO activity in polar configuration of these trilayers. The effect of the nanodisc array has been specified as the purely optical contribution and as the purely magneto-optical one [11]. In this paper, we study the film thickness effects of Au/Co/Au sandwiches and multilayers for MO-SPR sensors in the Kretschmann configuration to increase the sensor response related to an external magnetic field (Fig. 1).

2. Dielectric tensor for transverse configuration

The effects of magnetization on the relative permittivity tensor components are usually small and they can be expanded into series:

$$\varepsilon_{ij} = \varepsilon_{0, ij} + K_{ijk} M_k + G_{ijkl} M_k M_l + \dots = \varepsilon_{0, ij} + \varepsilon_{1, ij} + \varepsilon_{2, ij} + \dots \quad (1)$$

where $\varepsilon_{0, ij}$ are the permittivity components without magnetization in the crystal ($M = 0$), K_{ijk} are components of the third rank linear magneto-optical tensor describing linear dependence on the magnetization and G_{ijkl} are components of a fourth rank quadratic magneto-optical tensor characterizing quadratic dependence on the magneti-

zation. Since the quadratic contribution to the relative permittivity is generally small, the modeling has been focused on linear magneto-optical properties. For the transverse geometry in a linear approximation, the relative permittivity tensor is defined by [12]

$$\hat{\boldsymbol{\epsilon}}_T = \begin{bmatrix} \epsilon_0 & 0 & 0 \\ 0 & \epsilon_0 & -i\epsilon_l \\ 0 & i\epsilon_l & \epsilon_0 \end{bmatrix} = \epsilon_0 \begin{bmatrix} 1 & 0 & 0 \\ 0 & 1 & -iQ_T \\ 0 & iQ_T & 1 \end{bmatrix} \quad (2)$$

where

$$Q_T = \frac{\epsilon_l}{\epsilon_0} \quad (3)$$

is known as the Voigt parameter.

The chosen Cartesian system has the xy plane parallel to the planar system (x -axis is normal to the incidence plane); z -axis is normal to the structure.

3. Matrix formalism

The matrix formalism is an extremely useful form of describing the steady-state solution to Maxwell's equations subject to the boundary conditions imposed by isotropic and anisotropic multilayer stacks.

Electromagnetic fields at each boundary (see Fig. 1 showing the experimental set-up in this work: prism^(P)/Au⁽⁰⁾-film/Co⁽¹⁾-film/.../Au^(N-1)-film/halfspace^(N)) are obtained using the following partial products [9]:

$$\begin{aligned} \mathbf{M}^{(P, 0)} &= \left[\mathbf{D}^{(P)} \right]^{-1} \mathbf{D}^{(0)} \\ \mathbf{M}^{(0, 1)} &= \left[\mathbf{D}^{(0)} \right]^{-1} \mathbf{D}^{(1)} \\ \mathbf{M}^{(N-1, N)} &= \left[\mathbf{D}^{(N-1)} \right]^{-1} \mathbf{D}^{(N)} \end{aligned} \quad (4)$$

$\mathbf{D}^{(n)}$ denote the dynamic matrices, $n = 0, 1, \dots, N$. Thus, the total 4×4 (overall transfer) matrix \mathbf{M} describing the global reflection and transmission properties of the system can be expressed for normalized state as

$$\begin{aligned} \mathbf{M} &= \left[\mathbf{D}^{(P)} \right]^{-1} \mathbf{D}^{(0)} \mathbf{P}^{(0)} \left[\mathbf{D}^{(0)} \right]^{-1} \mathbf{D}^{(1)} \mathbf{P}^{(1)} \left[\mathbf{D}^{(1)} \right]^{-1} \dots \mathbf{D}^{(N-1)} \mathbf{P}^{(N-1)} \left[\mathbf{D}^{(N-1)} \right]^{-1} \mathbf{D}^{(N)} \\ &= \left[\mathbf{D}^{(P)} \right]^{-1} \mathbf{S}^{(0)} \mathbf{S}^{(1)} \dots \mathbf{S}^{(N-1)} \mathbf{D}^{(N)} \end{aligned} \quad (5)$$

where $\mathbf{S}^{(0)}$, $\mathbf{S}^{(1)}$, ..., $\mathbf{S}^{(N-1)}$ are the characteristic matrices of Au or Co films, and $\mathbf{P}^{(n)}$ is the matrix describing the propagation of plane waves between boundaries of the n -th medium. The characteristic matrix in the n -th medium can be written as

$$\mathbf{S}^{(n)} = \begin{bmatrix} S_{11}^{(n)} & S_{12}^{(n)} & S_{13}^{(n)} & S_{14}^{(n)} \\ S_{21}^{(n)} & S_{22}^{(n)} & S_{23}^{(n)} & S_{24}^{(n)} \\ S_{31}^{(n)} & S_{32}^{(n)} & S_{33}^{(n)} & S_{34}^{(n)} \\ S_{41}^{(n)} & S_{42}^{(n)} & S_{43}^{(n)} & S_{44}^{(n)} \end{bmatrix} \quad (6)$$

The isotropic region is specified by $\mathbf{S}^{(n)}$ matrix, the elements $S_{ij}^{(n)}$ of which are

$$S_{13}^{(n)} = S_{14}^{(n)} = S_{23}^{(n)} = S_{24}^{(n)} = S_{31}^{(n)} = S_{32}^{(n)} = S_{41}^{(n)} = S_{42}^{(n)} = 0$$

$$S_{11}^{(n)} = \frac{1}{2} \left[\exp(i\beta^{(n)}) + \exp(-i\beta^{(n)}) \right] = S_{22}^{(n)} = S_{33}^{(n)} = S_{44}^{(n)}$$

$$S_{12}^{(n)} = \frac{1}{2} \frac{\exp(i\beta^{(n)}) - \exp(-i\beta^{(n)})}{N^{(n)} \cos(\varphi^{(n)})} \quad (7)$$

$$S_{21}^{(n)} = \frac{1}{2} \left[N^{(n)} \cos(\varphi^{(n)}) \exp(i\beta^{(n)}) - N^{(n)} \cos(\varphi^{(n)}) \exp(-i\beta^{(n)}) \right]$$

$$S_{34}^{(n)} = \frac{1}{2} \left[-\frac{\cos(\varphi^{(n)})}{N^{(n)}} \exp(i\beta^{(n)}) + \frac{\cos(\varphi^{(n)})}{N^{(n)}} \exp(-i\beta^{(n)}) \right]$$

$$S_{34}^{(n)} = \frac{1}{2} \left[-\frac{N^{(n)}}{\cos(\varphi^{(n)})} \exp(i\beta^{(n)}) + \frac{N^{(n)}}{\cos(\varphi^{(n)})} \exp(-i\beta^{(n)}) \right]$$

where $\varphi^{(n)}$ is the angle of incidence and

$$N^{(n)} = n^{(n)} - ik^{(n)} \quad (8)$$

is the complex refractive index; $\beta^{(n)}$ is defined by ($t^{(n)}$ denotes the thickness of the n -th film):

$$\beta^{(n)} = \frac{\omega}{c} N^{(n)} t^{(n)} \cos(\varphi^{(n)}) \quad (9)$$

For an anisotropic case in the transverse geometry, the relatively single elements of characteristic matrices provide a valuable insight into the magnetic and optical behavior of the system. The characteristic matrices are block-diagonal in transverse geometry in the case of effects linear in magnetization [13]. In this special arrangement, the mode conversion is not observed and waves are traveling through the planar structure without polarization conversion. The matrix \mathbf{S} is described by the elements:

$$\begin{aligned}
 S_{11} &= \left[L_{11} \exp(i\beta_s) + L_{11} \exp(-i\beta_s) \right] |D|^{-1} \\
 S_{12} &= \left[-L_{12} \exp(i\beta_s) + L_{12} \exp(-i\beta_s) \right] |D|^{-1} \\
 S_{21} &= \left[D_{21} L_{11} \exp(i\beta_s) - D_{21} L_{11} \exp(-i\beta_s) \right] |D|^{-1} \\
 S_{22} &= \left[-D_{21} L_{12} \exp(i\beta_s) - D_{21} L_{12} \exp(-i\beta_s) \right] |D|^{-1} \\
 S_{33} &= \left[D_{33} L_{33} \exp(i\beta_p) - D_{33} L_{43} \exp(-i\beta_p) \right] |D|^{-1} \\
 S_{34} &= \left[D_{33} L_{34} \exp(i\beta_p) - D_{33} L_{34} \exp(-i\beta_p) \right] |D|^{-1} \\
 S_{43} &= \left[D_{43} L_{33} \exp(i\beta_p) - D_{44} L_{43} \exp(-i\beta_p) \right] |D|^{-1} \\
 S_{44} &= \left[D_{43} L_{34} \exp(i\beta_p) - D_{44} L_{34} \exp(-i\beta_p) \right] |D|^{-1} \\
 S_{13} &= S_{14} = S_{23} = S_{24} = S_{31} = S_{32} = S_{41} = S_{42} = 0
 \end{aligned} \tag{10}$$

where

$$\begin{aligned}
 |D| &= -2 D_{21} D_{33} (D_{44} - D_{43}) \\
 L_{11} &= -D_{21} D_{33} (D_{44} - D_{43}) \\
 L_{12} &= D_{33} (D_{44} - D_{43}) \\
 L_{33} &= -2 D_{21} D_{44} \\
 L_{34} &= 2 D_{21} D_{33} \\
 L_{43} &= 2 D_{21} D_{43}
 \end{aligned} \tag{11}$$

and

$$\begin{aligned}
 D_{21} &= N_{z1} \\
 D_{33} &= \varepsilon_0 - N_y^2
 \end{aligned} \tag{12}$$

$$D_{43} = -\left(-iN_y\epsilon_1 + N_{z3}\epsilon_0\right)$$

$$D_{44} = -\left(-iN_y\epsilon_1 + N_{z4}\epsilon_0\right)$$

The roots N_{zj} ($j = 1, \dots, 4$) are the solutions of the eigenvalue equation describing plane wave propagation in an anisotropic medium and are given by:

$$\begin{aligned} N_{z1} &= \left(\epsilon_0 - N_y^2\right)^{1/2} \\ N_{z2} &= -\left(\epsilon_0 - N_y^2\right)^{1/2} \\ N_{z3,4} &= \pm \left[\epsilon_0 \left(1 - Q_T^2\right) - N_y^2\right]^{1/2} \end{aligned} \quad (13)$$

with

$$\begin{aligned} \beta_s &= \frac{\omega}{c} N_{z1} t \\ \beta_p &= \frac{\omega}{c} N_{z3} t \end{aligned} \quad (14)$$

where s, p stand for s - and p -polarized light wave. The tangential component of the refractive index N_y is expressed as:

$$N_y = Na_y \quad (15)$$

where a_y is the complex direction cosine.

The anisotropy affects the solutions $N_{z3,4}$ of the eigenvalue equation for p -polarized waves, see (13). This dependence can be expressed with the help of the ratio:

$$\frac{N_z}{\Delta N_z} = \frac{N_z(0)}{N_z(0) - N_z(M)} \quad (16)$$

where $N_z(0)$ is the z -component of N_{z3} for isotropic case, while $N_z(M)$ is the z -component for the N_{z3} with magnetic field applied (induced anisotropy).

The relations between the amplitudes of the incident, transmitted and reflected waves, and the interaction of the plane electromagnetic wave with the structure are determined in terms of the M_{ij} ($i, j = 1, \dots, 4$) elements of the overall matrix \mathbf{M} [14]. In transverse magnetization (magnetization lies in the plane of the sample and is normal to the plane of incidence) [13]:

$$\begin{aligned}
r_{ssT} &= M_{21T}/M_{11T} \\
r_{ppT} &= M_{43T}/M_{33T} \\
t_{ssT} &= 1/M_{11T} \\
t_{ppT} &= 1/M_{33T} \\
r_{spT} = r_{psT} = t_{spT} = t_{pst} &= 0
\end{aligned} \tag{17}$$

In order to determine the amount of energy reflected from the boundary, one needs to consider a squared absolute value of the r_{pp} reflection coefficient:

$$R_{pp} = |r_{pp}|^2 \tag{18}$$

For the case without magnetization, isotropic media can be assumed, and the reflection and transmission coefficients can be described by well-known relations.

4. Numerical simulation

The MO effect produces in the transverse configuration (linear approximation only) a relative change of the reflectance R_{pp} of the p -polarized light:

$$\frac{\Delta R_{pp}}{R_{pp}} = \frac{R_{pp}(M) - R_{pp}(0)}{R_{pp}(0)} \tag{19}$$

where $R_{pp}(M)$ and $R_{pp}(0)$ denote reflectances with and without magnetization, respectively. We analyze the magneto-optical effects in the structures created by Au and Co thin films with the objective to maximize the value of $\Delta R_{pp}/R_{pp}$. The results are given for Au–Co sandwiches and multilayers. In the modeling we assume the Kretschmann experimental arrangement [15] with BK-7 prism ($\epsilon_p = 2.310$) and water as dielectric medium ($\epsilon_w = 1.775$). The value of the dielectric constant for Co has been chosen as $\epsilon_{Co,0} = -12.5040 + 18.4639i$ [16], the Voigt parameter of this ferromagnetic material is $Q = 0.03273 + 0.01092i$. The Au dielectric constant is $\epsilon_{Au} = -11.2376 + 1.2834i$ [17]. All the optical parameters listed are related to the wavelength of 632.8 nm. For the numerical simulations, the thickness of Co layers has been fixed to 2.7 nm.

First of all, the Fig. 2 shows the normalized dependence of real and imaginary parts of the fraction $N(z)/\Delta N(z)$ on the incidence angle for the Co layer with the above parameters. This graphic output demonstrates the induced anisotropy effects related to the root N_{z3} . In relation (16), the N_y is variable parameter. Its value is changed – in our case – from 0 to 1.520 as a function of the incidence angle. Considering the dielectric constant for Co, the absence of peak in the graphic outputs of real and imaginary parts of the fraction discussed is observed.

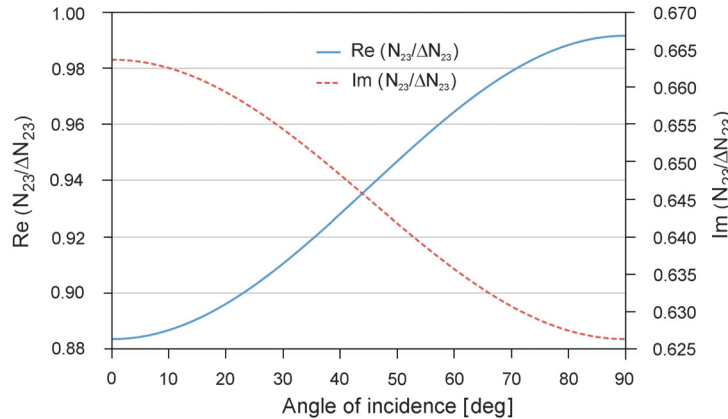


Fig. 2. Normalized dependence of real and imaginary parts of $N_z/\Delta N_z$ as the function of incidence angle for N_{z3} root.

The main attention has been focused on a SPR configuration with the Au–Co–Au sandwiches. In this case, the thickness of the gold layer attached directly to the prism base has a constant value of 29.4 nm in order to enable a comparison with [1] (see Fig. 3). The authors in [1] compare the theoretical MO effects in the transversal

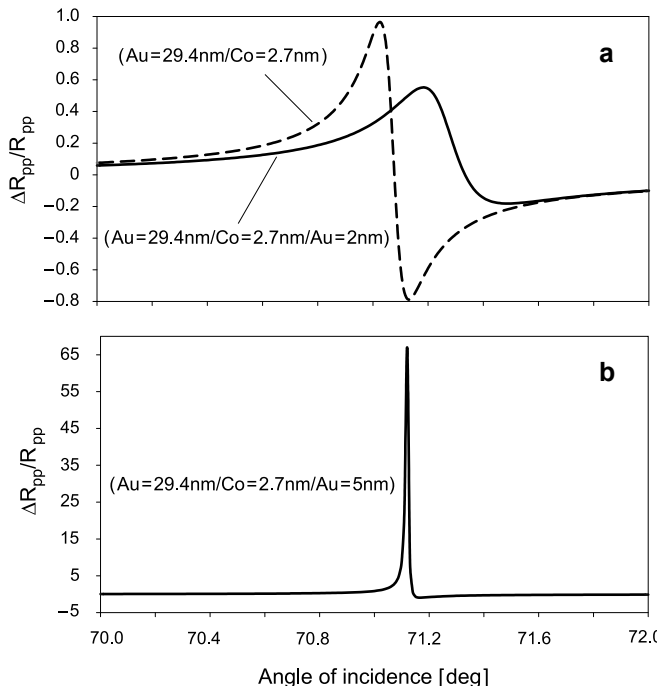


Fig. 3. The figures display thickness effect of Au underlying thin film of Au/Co/Au sandwiches on relative change of the reflectance.

configuration of magnetization for a Co layer of 20 nm to MO results of Co–Au double-layer composed of 10 nm of Co and 29.4 nm of Au. The metallic thicknesses have been chosen to maximize the sensitivity. The dashed line in Fig. 3a demonstrates the case where the gold underlying thin film originally in contact with the medium studied is not present. One can observe an explicit enhancement of the $\Delta R_{pp}/R_{pp}$ parameter for a setup without this noble metal layer. The question remains, however, whether this structure where the ferromagnetic Co film is not protected, is practically applicable. The optimization of the MO-SPR sandwich is shown in Fig. 3b. A relatively small change of the protected gold film thickness (from 2 nm to 0.5 nm, see Figs. 3a and 3b) creates a large amplitude shift of resonance maximum. The coefficient ΔR_{pp} in transverse configuration is proportional to TM electric field components only (see (13)). It can be expected that the optimization of ΔR_{pp} corresponds to the high-quality surface plasmon resonance [5]. The ΔR_{pp} analysis realized for the thin film structure specified in Fig. 3b indicates the ΔR_{pp} maximum of 3.65×10^{-3} for the incidence angle of 68.65° . The minimum of $R_{pp}(0)$ is located at incidence angle of 70.89° . It means that the relative change of reflectance described in Fig. 3b is importantly affected by $R_{pp}(0)$ distribution. The authors in [5] demonstrate a weak dependence of ΔR_{pp} as a function of underlying gold layer. For our structure depicted in Fig. 3a (BK-7/Au = 29.4 nm/Co = 2.7 nm/Au = 2 nm/water) the maximum of ΔR_{pp} achieves the value of 3.59×10^{-3} at the incidence angle of 68.16° . For the last system discussed the minimum of $R_{pp}(0)$ has been found at 71.05° . We can see the undersized shifts of the maximal values of ΔR_{pp} and their positions as a function of incidence angle and positions of $R_{pp}(0)$ minima play the dominant role for $\Delta R_{pp}/R_{pp}$ response (see Fig. 3).

The influence of the thin films sequence on the prism base is also of interest here. Figure 4 demonstrates this effect (BK-7/Au/Co/H₂O versus BK-7/Co/Au/H₂O), with all other parameters the same. Locating the Co thin film directly on the prism base (BK-7/Co/Au/H₂O) causes an important reduction of the MO-SPR sensor magnetic response (compare Fig. 4 and Fig. 3a). The magneto-optical medium (Co thin film) placement directly on coupling prism base blocks off the surface plasmon resonance.

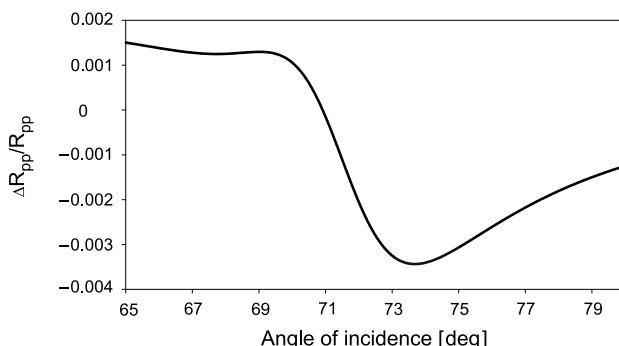


Fig. 4. The influence of thin films sequence on prism base – BK-7/Co = 2.7 nm/Au = 29.4 nm/H₂O structure (compare Fig. 3a).

The total thickness of the Au–Co structure plays a very important role as regards the $\Delta R_{pp}/R_{pp}$ dependence on incidence angle. This situation is documented by a thin layer system Au–Co–Au, where the thickness of the Au film located directly on the prism base is varied, while other films have fixed parameters. This strong impact of a thickness change of the Au layer from 29.4 nm to 26.4 nm is illustrated in Fig. 5. The setting Au = 27.4 nm/Co = 2.7 nm/Au = 6 nm (Fig. 5b) generates a state with a maximum value of the resonance peak. Reducing the gold thin film thickness to 26.4 nm decreases the sensor response in the range of two orders of magnitude. The invariable thickness of the underlying 6 nm Au thin film in the sandwich Au–Co–Au structure has been chosen to have an option of thickness variation of Au film directly located on the prism base. In [5], the effect of Au film thickness alteration for Au–Co–Au SPR sandwiches is analyzed. For transverse orientation and the case where the thickness of Au film directly located on prism base is fixed (coupling prism/Au = 17.9 nm/Co = 5.7 nm/Au(v) – variable thickness) in the frame of ΔR_{pp} optimization the following values of ΔR_{pp} have been achieved: Au (v = 0.5 nm) – $\Delta R_{pp} = 3.67 \times 10^{-3}$, Au (v = 6 nm) – $\Delta R_{pp} = 3.29 \times 10^{-3}$ [5]. Our value of ΔR_{pp} for the structure BK-7/Au = 27.4 nm/Co = 2.7 nm/Au = 6 nm (Fig. 5b) has been specified with the help of TM modeling and achieved 3.14×10^{-3} . It means about 4.5% reduction in comparison with the state described in [5] (prism/Au = 17.9 nm/Co = 5.7 nm/Au = 6 nm).

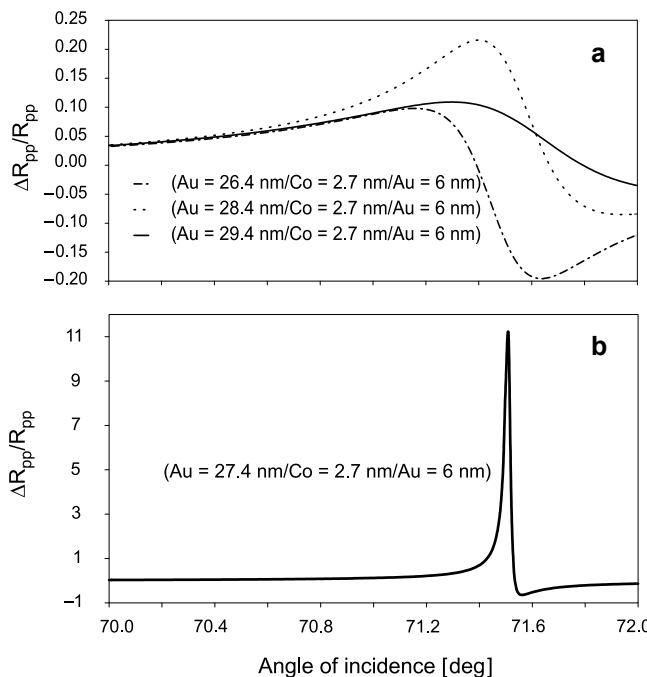


Fig. 5. The figures display thickness effect of Au top thin film of Au/Co/Au sandwiches on relative change of the reflectance.

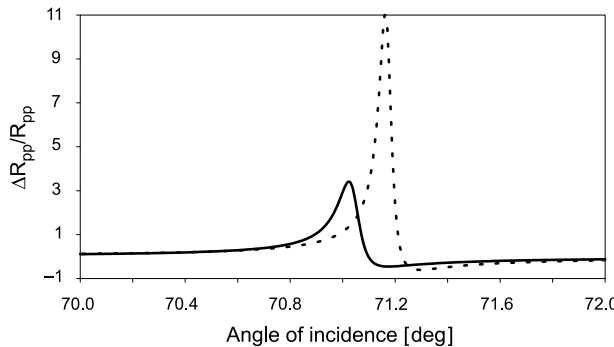


Fig. 6. The effect of Co–Au double layer on magneto-optical response: Co–Au double layer has been applied twice ($\text{Au} = 19 \text{ nm}/(\text{Co} = 2.7 \text{ nm}/\text{Au} = 2.7 \text{ nm}) \times 2$) – solid line, Co–Au double layer has been applied three times ($\text{Au} = 11.45 \text{ nm}/(\text{Co} = 2.7 \text{ nm}/\text{Au} = 2.7 \text{ nm}) \times 3$) – dashed line.

The role of multilayers for a MO-SPR effect enhancement has been investigated by applying a Co–Au bi-layer (with the same thickness of these films $t_{\text{Co}} = t_{\text{Au}} = 2.7 \text{ nm}$). The solution has been optimized by varying the thickness of the Au top thin film contacting the BK-7 prism. The results of this approach are illustrated in Fig. 6. For the system with $\text{prism}/\text{Au} = 11.45 \text{ nm}/(\text{Co} = 2.7 \text{ nm}/\text{Au} = 2.7 \text{ nm}) \times 3$, the maximum of response has been achieved. For these multilayered structures the quality of surface plasmon resonance has been studied by ΔR_{pp} analysis [5]. The resonant coupling of the gold surface plasmons with the p -component of the light electric field has been specified by a 4×4 matrix algebra [13, 18]. Considering $\text{prism}/\text{Au} = 11.45 \text{ nm}/(\text{Co} = 2.7 \text{ nm}/\text{Au} = 2.7 \text{ nm})^3/\text{water}$ system the ΔR_{pp} value of 5×10^{-3} at incidence angle of 67.11° has been achieved. In the previous structure (Fig. 5b) the lower level of ΔR_{pp} (3.14×10^{-3}) has been demonstrated. However, the effect of $R_{pp}(0)$ in our multilayered configuration has to be considered – its distribution as a function of incidence angle and its value at minimum play the dominant role for $\Delta R_{pp}/R_{pp}$ response.

5. Conclusions

For the transverse orientation (in linear approximation), the response of $\Delta R_{pp}/R_{pp}$ is analyzed by a 4×4 matrix algebra. The application of Au/Co/Au sandwiches for MO-SPR sensors enables one to modify the $\Delta R_{pp}/R_{pp}$ value. The optimization of sandwich layer thicknesses (*i.e.*, prism/Au = 29.4 nm/Co = 2.7 nm/Au = 0.5 nm) leads to a significant enhancement of the $\Delta R_{pp}/R_{pp}$ parameter. Changing the gold thin film thickness of the layer, originally in contact with the medium studied, from 2 nm to 0.5 nm enhances the responsivity by about two orders of magnitude. The ΔR_{pp} coefficient in transverse configuration is proportional to TM electric field components only. It can be expected that the optimization of ΔR_{pp} corresponds to the high-quality surface plasmon resonance. A detail analysis of the relative change of reflectance

$(\Delta R_{pp}/R_{pp})$ demonstrated the important influence of $R_{pp}(0)$. The undersized shifts of the maximal values of ΔR_{pp} and their positions as a function of incidence angle and the positions of $R_{pp}(0)$ minima play the dominant role for $\Delta R_{pp}/R_{pp}$ response. One approach in the optimization process is the application of multilayers. It has been shown that an appropriate combination of double layers can improve the magneto-optical response of the MO-SPR. However, the influence of $R_{pp}(0)$ distribution as a function of incidence angle and its value at minimum has to be considered. In conclusion, the optimization of the MO-SPR sensor depends on the accurate control of the thicknesses of noble metal and magneto-optical thin films forming the sensing unit, the magneto-optical coefficients of applied ferromagnetic layer, and $R_{pp}(0)$ values for the concrete MO-SPR structure.

Acknowledgments – This work has been partially supported by grant #CZ.1.05/2.1.00/01.0040 and by the Ministry of Education, Youth and Sport of the Czech Republic (#MSM 6198910016).

References

- [1] SEPÚLVEDA B., CALLE A., LECHUGA L.M., ARMELLES G., *Highly sensitive detection of biomolecules with the magneto-optic surface-plasmon-resonance sensor*, Optics Letters **31**(8), 2006, pp. 1085–1087.
- [2] NARAYANASWAMY R., WOLFBEIS O.S., *Optical Sensors*, Springer-Verlag, Berlin, 2004, p. 421.
- [3] RIGHINI G.C., TAJANI A., CUTOLO A., *An Introduction to Optoelectronic Sensors*, Series in Optics and Photonics – Vol. 7, World Scientific, Singapore, 2009.
- [4] SEPÚLVEDA B., LECHUGA L.M., ARMELLES G., *Magneto-optic effects in surface-plasmon-polaritons slab waveguides*, Journal of Lightwave Technology **24**(2), 2006, pp. 945–955.
- [5] BONOD N., REINISCH R., POPOV E., NEVIÈRE M., *Optimization of surface-plasmon-enhanced magneto-optical effects*, Journal of the Optical Society of America B **21**(4), 2004, pp. 791–797.
- [6] LUKASZEW R.A., CLAVERO C., WINCHESKI R., YANG K., SKUZA J.R., *Magneto-optically enhanced surface plasmon resonance*, MMM Conference, Book of Abstracts, 2008, p. 359.
- [7] UCHIDA H., MASUDA Y., FUJIKAWA R., BARYSHEV A.V., INOUE M., *Large enhancement of Faraday rotation by localized surface plasmon resonance in Au nanoparticles embedded in Bi:YIG film*, Journal of Magnetism and Magnetic Materials **321**(7), 2009, pp. 843–845.
- [8] FERREIRO VILA E., BENDANA SUEIRO X.M., GONZALEZ-DÍAZ J.B., GARCIA-MARTÍN A., GARCIA-MARTÍN J.M., CEBOLLADA NAVARRO A., ARMELLES REIG G., MENESES RODRIGUEZ D., MUÑOZ SANDOVAL E., *Surface plasmon resonance effects in the magneto-optical activity of Ag–Co–Ag trilayers*, IEEE Transactions on Magnetics **44**(11), 2008, pp. 3303–3306.
- [9] GONZÁLES-DÍAZ J.B., GARCÍA-MARTÍN A., ARMELLES G., GARCÍA-MARTÍN J.M., CLAVERO C., CEBOLLADA A., LUKASZEW R.A., SKUZA J.R., KUMAH D.P., CLARKE R., *Surface-magnetoplasmon nonreciprocity effects in noble-metal/ferromagnetic heterostructures*, Physical Review B **76**(15), 2007, p. 153402.
- [10] SAFAROV V.I., KOSOBUKIN V.A., HERMANN C., LAMPEL G., PERETTI J., MARLIERE C., *Magneto-optical effects enhanced by surface plasmons in metallic multilayer films*, Physical Review Letters **73**(26), 1994, pp. 3584–3587.
- [11] ARMELLES G., GONZÁLES-DÍAZ J.B., GARCÍA-MARTÍN A., GARCÍA-MARTÍN J.M., CEBOLLADA A., GONZÁLES M.U., ACIMOVIC S., CESARIO J., QUIDANT R., BADENES G., *Localized surface plasmon resonance effects on the magneto-optical activity of continuous Au/Co/Au trilayers*, Optics Express **16**(20), 2008, pp. 16104–16112.

- [12] VIŠŇOVSKÝ Š., YAMAGUCHI T., PIŠTORA J., POSTAVA K., BEAUVILLAIN P., GOGOL P., *Unidirectional propagation in planar optical waveguides*, Schenk, Ostrava, 2006, p. 82.
- [13] VIŠŇOVSKÝ Š., *Magneto-optical ellipsometry*, Czechoslovak Journal of Physics B **36**(5), 1986, pp. 625–650.
- [14] YEH P., *Optical Waves in Layered Media*, Wiley, New York, 1988.
- [15] NUSTER R., PALTAUF G., BURGHOLZER P., *Comparison of surface plasmon resonance devices for acoustic wave detection in liquid*, Optics Express **15**(10), 2007, pp. 6087–6095.
- [16] PALIK E.D., *Handbook of Optical Constants of Solids II*, Academic Press, San Diego, 1991.
- [17] JOHNSON P.B., CHRISTY R.W., *Optical constants of the noble metals*, Physical Review B **6**(12), 1972, pp. 4370–4379.
- [18] PIŠTORA J., POSTAVA K., ŠEBESTA R., *Optical guided modes in sandwiches with ultrathin metallic films*, Journal of Magnetism and Magnetic Materials **198–199**, 1999, pp. 683–685.

Received December 16, 2009
in revised form March 15, 2010